https://doi.org/10.1590/jatm.v14.1255

ORIGINAL PAPER

Design of the Missile Attitude Controller Based on the Active Disturbance Rejection Control

Shanzhong Liu[1*], Mengqi Xue [1], Yaolong Qiu[1], Xingyu Zhou[1], Qingxiu Zhao[1]

1. Henan University of Science and Technology – School of Information Engineering – Luoyang, Henan – China

*Correspondence author: szliu@haust.edu.cn

ABSTRACT

Targeting at the stable tracking control problem of the interceptor missile's flight attitude in the terminal guidance phase, the nonlinear mathematical model of missile attitude is used as the research object, in which the coupling among the channels is considered. The control strategies of Proportion Differentiation (PD) control, nonlinear and linear active disturbance rejection control are studied. Firstly, the expanded state observer is designed to estimate the total disturbance information in real time, and the error feedback controller is designed to provide disturbance compensation, so that the original second-order nonlinear system is decoupled into the canonical form of cascade integrators to realize the stable tracking control of the missile attitude. Secondly, the three-channel coupling closed-loop control system model is established, and under the influence of external disturbance and model parameter perturbation, the comparison between the three control methods is demonstrated by simulations. The simulation results show that these three methods can stabilize the missile attitude and track the reference input signal. Among them, the nonlinear active disturbance rejection control has the smallest overshoot, the strongest anti-interference ability, and better robustness.

Keywords: Attitude control; Active Disturbance Rejection Control; Extended state observer; Robustness.

INTRODUCTION

In the modern battlefield, with the continuous improvement of the performance of ballistic missile weapons, the requirements for the interception accuracy and response speed of antimissile interception missiles should be higher and higher. When the interceptor missile enters the terminal guidance phase, in order to search for the target, the attitude of the missile often needs to be adjusted quickly to track and intercept the target. Therefore, it is particularly important to design high-precision and fast-response attitude controllers to improve the success rate of the interceptor missile hitting the target.

However, during the flight of the interceptor missile, due to the changes of aerodynamics and external battlefield environment, system parameters are uncertain and the mathematical model of the missile is difficult to be established accurately. Hence, it is required that the design of the controller not only does not rely heavily on the model information, but also ensures the

Received: Dec. 16, 2021 | **Accepted:** Mar. 21, 2022
Peer Review History: Single Blind Peer Review.
Section editor: Luiz Martins-Filho

robustness. In this regard, many scholars have done a lot of researches. Chen *et al.* (2012) have used the classical Proportion Integration Differentiation (PID) control which does not require high accuracy of the controlled object model to control each subchannel of the missile, so that each subchannel can meet the requirements of real-time control. Liu *et al.* (2019) have provided a neural network weight adjustment formula by combining PID control with reinforcement learning technology, which is not based on the controlled object model but only depends on the observation data.

The proposed formula has realized the online closed-loop self-adaptive tuning of parameters. In literature (Basha *et al.* 2017), the robust PID controller based on the disturbance observer has been used for yaw and pitch autopilots. At the same time, the fuzzy PID controller based on the disturbance observer has been used for roll autopilot. The designed control strategy has reduced the impact of disturbance on the system greatly. Li *et al.* (2020) have adopted PID control combining with depth deterministic strategy gradient algorithm to achieve higher precision and faster target tracking control. The tracking commands and their first-order differential signals of the inner loop have been obtained by using the extended state observer and command filtering method, which makes the system have good robustness (Xu *et al.* 2018). Targeting at the robustness of engineering control, an Active Disturbance Rejection Control (ADRC) technique based on the extended state observer has been proposed (Han 2002). ADRC technique is an improvement on PID, which does not rely on the model of the controlled object and relies on errors elimination errors. Meanwhile, it overcomes the shortcoming that PID differential signal is not easy to extract, and it solves the contradiction between PID rapidity and overshoot.

On the basis of ADRC, Linear Active Disturbance Rejection Control (LADRC), as a new controller design method, has been proposed by Gao (2003), who make it easier to adjust the parameters. Yuan *et al.* (2013) and Z. Chen *et al.* (2013) have illustrated the feasibility of LADRC by analyzing and verifying the approach. In recent years, ADRC has been gradually and successfully applied to the control of various equipment, such as permanent magnet synchronous motor (Sun *et al.* 2020), ship steering (Li *et al.* 2018), flight control (Lu *et al.* 2020), etc. Under all of the above circumstances, ADRC has shown superior control performance.

From the results of literature research, although the classical PID control does not have high requirements on the accuracy of the controlled object model, its ability to attenuate overshoot and measure noise is insufficient. It is not easy to meet the high-performance control requirements. However, Nonlinear Active Disturbance Rejection Control (NLADRC) and LADRC are an improvement of the classical PID control, which has obvious effects on improving the robustness and stability of the system. It is suitable for solving the control problems of coupling systems with disturbance and uncertainty. Therefore, in this paper, aiming at the flight attitude control problem of interceptor missile in the terminal guidance phase, the mathematical model of three-channel coupled attitude is used as the research object. The Proportion Differentiation (PD), nonlinear and linear active disturbance rejection controllers are designed with PD control, NLADRC and LADRC, respectively, and the control performances of the three control algorithms are compared through simulation analysis.

ESTABLISHMENT OF MATHEMATICAL MODEL

Most interceptor missiles are axisymmetric bodies. In the process of flight, they have the characteristics of variable mass, variable shape, and elastic or plastic deformation. As a result, their motion equations are very complicated. When establishing the mathematical equation for the interceptor's attitude, the following assumptions are made: (1) regarding the interceptor as a rigid body with constant mass; (2) omitting some secondary factors that affect the movement of the interceptor, such as the rotation of the Earth, atmospheric environment, gravity, etc. The mathematical equation of the interceptor's attitude is established based on Euler attitude angle, which is described as follows (Zhou 2002):

According to the theorem on the moment of momentum, the dynamic equation of the projectile body rotating around the center of mass is given by Eq. 1:

$$\begin{cases} J_x \dfrac{d\omega_x}{dt} + (J_z - J_y)\omega_z\omega_y = M_x \\ J_y \dfrac{d\omega_y}{dt} + (J_x - J_z)\omega_x\omega_z = M_y \\ J_z \dfrac{d\omega_z}{dt} + (J_y - J_x)\omega_x\omega_y = M_z \end{cases} \tag{1}$$

According to the relationship between the attitude angle and the angular velocity, the kinematic equation of the projectile body moving around the center of mass is given by Eq. 2:

$$\begin{cases} \dfrac{d\vartheta}{dt} = \omega_y \sin\gamma + \omega_z \cos\gamma \\ \dfrac{d\varphi}{dt} = (\omega_y \cos\gamma - \omega_z \sin\gamma) / \cos\vartheta \\ \dfrac{d\gamma}{dt} = \omega_x - \tan\vartheta(\omega_y \cos\gamma - \omega_z \sin\gamma) \end{cases} \tag{2}$$

By combining Eq. 1 and Eq. 2, the attitude mathematical model of the three-channel coupling is obtained (Eq. 3):

$$\begin{cases} \ddot{\vartheta} = \dfrac{(J_x - J_y)}{J_z}\omega_x\omega_y \cos\gamma + \dot{\omega}_y \sin\gamma + (\omega_y\cos\gamma - \omega_z \sin\gamma)\dot{\gamma} + \dfrac{\cos\gamma}{J_z} M_z \\ \ddot{\varphi} = \dfrac{(J_z - J_x)\cos\gamma}{J_y \cos\vartheta}\omega_z\omega_x - \dfrac{\sin\gamma}{\cos\vartheta}\dot{\omega}_z + \dfrac{\dot{\vartheta}\cos\gamma\sin\vartheta - \dot{\gamma}\sin\gamma\cos\vartheta}{\cos^2\vartheta}\omega_y \\ \quad - \dfrac{\dot{\gamma}\cos\gamma\cos\vartheta + \dot{\vartheta}\sin\gamma\sin\vartheta}{\cos^2\vartheta}\omega_z + \dfrac{\cos\gamma}{J_y\cos\vartheta}M_y \\ \ddot{\gamma} = -\dot{\vartheta}\sec^2\vartheta(\omega_y\cos\gamma - \omega_z\sin\gamma) - \tan\vartheta(\dot{\omega}_y\cos\gamma - \omega_y\dot{\gamma}\sin\gamma) \\ \quad + \tan\vartheta(\dot{\omega}_z \sin\gamma + \omega_z\dot{\gamma}\cos\gamma) + \dfrac{J_y - J_z}{J_x}\omega_y\omega_z + \dfrac{1}{J_x}M_x \end{cases} \tag{3}$$

where γ, ϑ, and φ are the roll angle, the pitch angle, and the yaw angle, respectively; ω_x, ω_y, and ω_z are the roll angular velocity, the yaw angular velocity, and the pitch angular velocity, respectively; J_x, J_y, and J_z are the moments of inertia; M_x, M_y, and M_z are the roll moments, the yaw moments, and the pitch moments, respectively. Particularly, in order to avoid the singularity of the equation, the pitch angle satisfies $\vartheta \neq 90°$.

ACTIVE DISTURBANCE REJECTION CONTROL METHOD

Nonlinear Active Disturbance Rejection Control

The main idea of NLADRC (Han 2008) is to define a generalized disturbance concept: total disturbance, including internal disturbance and external disturbance, which is estimated indiscriminately through the extended state observer, and fed back to the system. Then the original system is transformed into the canonical form of cascade integrators to realize the stable tracking control. NLADRC consists of four parts: tracking differentiator, extended state observer, feedback control and disturbance compensation. Its structure diagram is shown in Fig. 1.

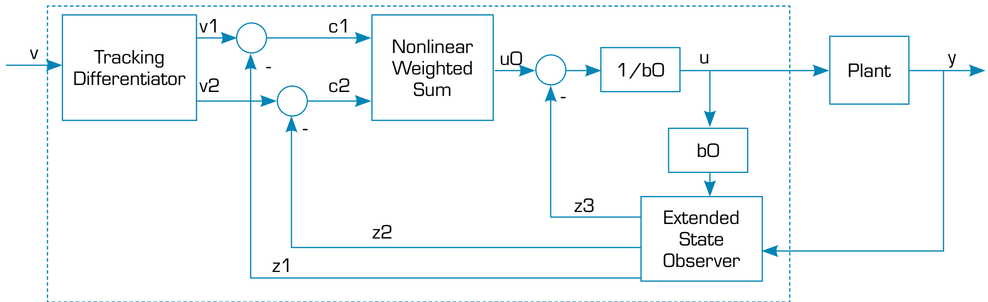

Figure 1. Structure diagram.

TRACKING DIFFERENTIATOR

The tracking differentiator is a single-input and dual-output module. It arranges the transition process for the reference input, which is convenient for real-time tracking and extracting the differential signal, and calculating the differential error. It can improve the control performance effectively. The common tracking differentiator is shown in Eq. 4.

$$\begin{cases} v_1(k+1) = v_1(k) + hv_2(k) \\ v_2(k+1) = v_2(k) + hfst(v_1(k) - v(k), v_2(k), \delta, h) \end{cases} \tag{4}$$

where h is the sampling period, $v(k)$ is the input at time k, δ is the parameter that determines the speed of tracking, and $fst(\cdot)$ is the comprehensive function of the fastest control as shown in Eq. 5.

$$fst(x_1, x_2, \delta, h) = \begin{cases} -\delta \,\mathrm{sgn}(a), |a| > d \\ -\delta \dfrac{a}{d}, |a| \le d \end{cases}$$
$$a = \begin{cases} x_2 + \dfrac{a_0 - d}{2} \mathrm{sgn}(y), |y| > d_0 \\ x_2 + \dfrac{y}{h}, |y| \le d_0 \\ d = \delta h \\ d_0 = hd \\ y = x_1 + hx_2 \\ a_0 = \sqrt{d^2 + 8\delta |y|} \end{cases} \tag{5}$$

In this paper, the step signal with amplitude of 10 is used as the reference input signal, $h = 0.001$, $\delta = 15$. The processing result of the tracking differentiator is shown in Fig. 2.

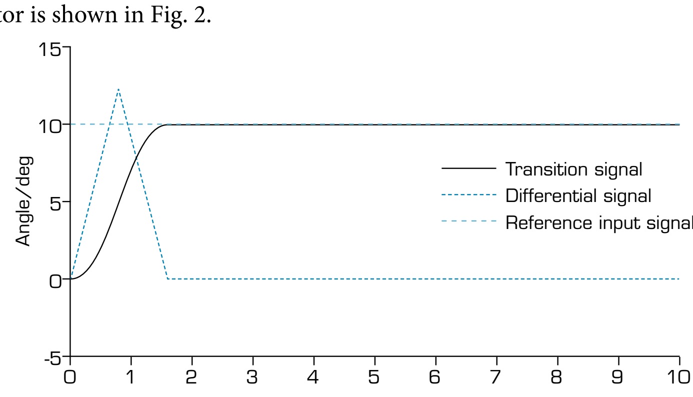

Figure 2. Output rendering of tracking differentiator.

NONLINEAR EXTENDED STATE OBSERVER

For the second-order nonlinear system model (Eq. 6):

$$\begin{cases} \dot{x}_1 = x_2 \\ \dot{x}_2 = f(x_1, x_2, w(t), t) + bu \\ y = cx_1 \end{cases} \tag{6}$$

where x_1, x_2 are state variables, y is the system output, u is the control input, and $f(x_1, x_2, w(t), t)$ is the comprehensive disturbance. Let the comprehensive disturbance be a new state variablex_3, and a nonlinear extended state observer is designed as Eq. 7.

$$\begin{cases} e = z_1 - y \\ \dot{z}_1 = z_2 - \beta_1 e \\ \dot{z}_2 = z_3 - \beta_2 fal(e, \alpha_1, \delta) + bu \\ \dot{z}_3 = -\beta_3 fal(e, \alpha_2, \delta) \end{cases}$$
$$fal(e, \alpha, \delta) = \begin{cases} \dfrac{e}{\delta^{\alpha-1}}, |e| \le \delta \\ |e|^{\alpha} \operatorname{sgn}(e), |e| > \delta \end{cases} \tag{7}$$

where z_1, z_2, and z_3 are the observer state variables, which are used to estimate the system state variables x_1, x_2, and x_3, respectively; β_1, β_2, and β_3 are the observer gains, fal(e, α , δ) is a nonlinear function, and δ is the interval length of the linear segment of the function.

NONLINEAR FEEDBACK AND DISTURBANCE COMPENSATION

Nonlinear feedback is a dual-input and single-output module. The input signals are the error and the differential error between the command signal and the output signal from observer respectively. The command signal and its differential signal are generated by the tracking differentiator. The nonlinear feedback controller is designed as Eq. 8.

$$\begin{cases} e_1 = v_1 - z_1 \\ e_2 = v_2 - z_2 \\ u_0 = k_p fal(e_1, \alpha_1, \delta) + k_d fal(e_2, \alpha_2, \delta) \end{cases} \tag{8}$$

where k_p, k_d are feedback parameters,u_0 is the virtual control quantity, $0 < \alpha_1 < 1 < \alpha_2$.

The disturbance compensation is designed according to the estimated value of the comprehensive disturbance, as shown in Eq. 9.

$$u = \frac{u_0 - z_3}{b_0} \tag{9}$$

Then the second-order nonlinear system model (Eq. 6) is decoupled into the canonical form of cascade integrators (Eq. 10), and the design of the whole control system is completed.

$$\begin{cases} \dot{x}_1 = x_2 \\ \dot{x}_2 = u_0 \\ y = cx_1 \end{cases} \tag{10}$$

LINEAR ACTIVE DISTURBANCE REJECTION CONTROL

LADRC is an improvement of NLADRC. It connects the parameters that need to be adjusted with the bandwidth of the observer and controller, and the poles are arranged in the same position uniformly, which greatly reduces the difficulty of parameter adjustment.

For the second-order nonlinear system model (Eq. 6), the linear observer is designed according to the Luenberger state observer theory (Eq. 11):

$$\dot{z} = Az + Bu - G(z_1 - y) \tag{11}$$

where $z = [z_1\ z_2\ z_3]^T$ is the observer state variable, and z_1, z_2 and z_3 are used to estimate the system state variables x_1, x_2, and x_3, respectively. $G = [k_1\ k_2\ k_3]^T$ is the observer gain matrix, $A = \begin{bmatrix} 0 & 1 & 0 \\ 0 & 0 & 1 \\ 0 & 0 & 0 \end{bmatrix}, B = \begin{bmatrix} 0 \\ b_0 \\ 0 \end{bmatrix}$.

If the poles of the characteristic equation are placed at the position of $-\omega_0$, the observer gain matrix is $G = [3\omega_0\ 3\omega_0^2\ 3\omega_0^3]^T$. In this way, the observer gain matrix is only related to the observer bandwidth, and it is easier to design the observer. The same as NLADRC, the disturbance compensation is designed as Eq. 12, and the linear feedback controller is designed as Eq. 13.

$$u = \frac{u_0 - z_3}{b_0} \tag{12}$$

$$u_0 = k_p(v - z_1) - k_d z_2 \tag{13}$$

where v is the reference input signal, k_p, k_d are controller gains. If the poles of the controller are placed at the position of $-\omega_c$, then $k_p = \omega_c^2$, $k_d = 2\omega_c$.

DESIGN OF ACTIVE DISTURBANCE REJECTION CONTROLLER

For the attitude mathematical model (Eq. 3), according to the ADRC method, the other terms except the control quantity torque are regarded as the total disturbance of the system and classified into the nonlinear function, as shown in Eq. 14.

$$\begin{cases} \ddot{\vartheta} = \dfrac{\cos\gamma}{J_z} M_z + f_1(\bullet) \\ \ddot{\varphi} = \dfrac{\cos\gamma}{J_y \cos\vartheta} M_y + f_2(\bullet) \\ \ddot{\gamma} = \dfrac{1}{J_x} M_x + f_3(\bullet) \end{cases} \tag{14}$$

where $x = [\gamma\ \vartheta\ \varphi]^T$ is the output quantity, $u = [M_z, M_z, M_z]^T$ is the control quantity, and the control quantity system matrix is

$$B = \begin{bmatrix} \dfrac{\cos\gamma}{J_z} & 0 & 0 \\ 0 & \dfrac{\cos\gamma}{J_y \cos\vartheta} & 0 \\ 0 & 0 & \dfrac{1}{J_x} \end{bmatrix}.$$

The structural block diagram of the whole system is shown in Fig. 3.

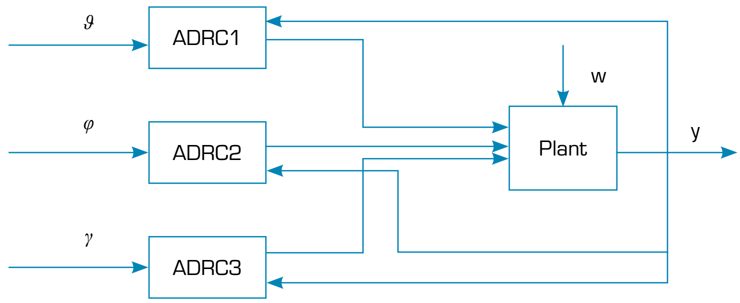

Figure 3. System structure block diagram.

DESIGN OF NONLINEAR ACTIVE DISTURBANCE REJECTION CONTROLLER

A nonlinear extended state observer is designed for Eq. 14, as shown in Eq. 15. The observer state variables z_{i1}, z_{i2} and z_{i3} are used to estimate the system state variables x_{i1}, x_{i2}, and x_{i3}, respectively.

$$\begin{cases} e_i = z_{i1} - x_i \\ \dot{z}_{i1} = z_{i2} - \beta_{i1} e_i \\ \dot{z}_{i2} = z_{i3} - \beta_{i2} fal(e_i, \alpha_1, \delta) + B(i,:)u \\ \dot{z}_{i3} = -\beta_{i3} fal(e_i, \alpha_2, \delta) \end{cases} \tag{15}$$

The feedback controller is designed according to the output signal of the tracking differentiator (Eq. 16).

$$\begin{cases} e_{i1} = v_{i1} - z_{i1} \\ e_{i2} = v_{i2} - z_{i2} \\ u_{i0} = k_{ip} fal(e_{i1}, \alpha_1, \delta) + k_{id} fal(e_{i2}, \alpha_2, \delta), 0 < \alpha_1 < 1 < \alpha_2 \end{cases} \tag{16}$$

The disturbance compensation is designed according to the estimated value of the comprehensive disturbance, as shown in Eq. 17.

$$u_i = \frac{u_{i0} - z_{i3}}{b_{i0}} \tag{17}$$

Then the mathematical model (Eq. 14) is decoupled into the canonical form of cascade integrators (Eq. 18), and the design of the whole control system is completed.

$$\begin{cases} \ddot{\vartheta} = u_{10} \\ \ddot{\varphi} = u_{20} \\ \ddot{\gamma} = u_{30} \end{cases} \tag{18}$$

DESIGN OF LINEAR ACTIVE DISTURBANCE REJECTION CONTROLLER

A linear extended state observer is designed for Eq. 14, as shown in Eq. 19.

$$\begin{cases} \dot{z}_{i1} = z_{i2} - k_{i1}(z_{i1} - x_i) \\ \dot{z}_{i2} = z_{i3} - k_{i2}(z_{i1} - x_i) + B(i,:)u \\ \dot{z}_{i3} = -k_{i3}(z_{i1} - x_i) \end{cases} \tag{19}$$

where $k_{i1}=3\omega_{i0}, k_{i2}=3\omega_{i0}^2, k_{i3}=\omega_{i0}^3$, the disturbance compensation is $u_i=\frac{u_{i0}-z_{i3}}{b_{i0}}$, and the virtual control quantity is $u_{i0}=k_{ip}(v_i-z_{i1})-k_{id}z_{i2}$.

SIMULATION RESEARCH

The intelligent control laboratory is mainly used for the semiphysical simulation test of precision guided weapon systems, in which lays the foundation for the success of missile flight test. The physical objects of the simulation test are mainly the three-axis turntable and the cabinet. The three-axis turntable has the function of three-axis speed and three-axis position, which is used to simulate the attitude change of the missile during flight, and the cabinet is used to support the operation of the simulation subsystem.

The missile parameters of the simulation model of the intelligent control laboratory are as follows: the initial mass of launch is m = 255 kg, the moments of inertia are J_x = 3.45 kg·m², $J_z = J_y$ = 60.85 kg·m², the missile diameter is d = 0.299 m. In this paper, taking the missile parameters of simulation model of the intelligent control laboratory as an example, and MATLAB is used for numerical simulation to compare the response curve of the three control methods.

The initial state of the interceptor missile attitude control system model is $\vartheta_0 = 0$, $\varphi_0 = 0$, and $\gamma_0 = 0$, the reference input signals are $\vartheta_r = 10$, $\varphi_r = 10$, and $\gamma_r = 0$.

- Verifying the control performance of the controller.

When the influence of external disturbance and parameter perturbation is not considered, the simulation results of three channels are shown in Figs. 4, 5 and 6. And the three control algorithms are compared, as shown in Table 1.

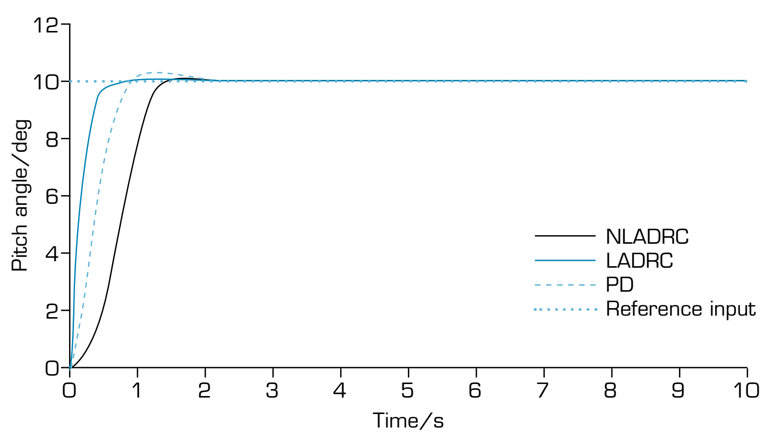

Figure 4. Response curve of pitch channel.

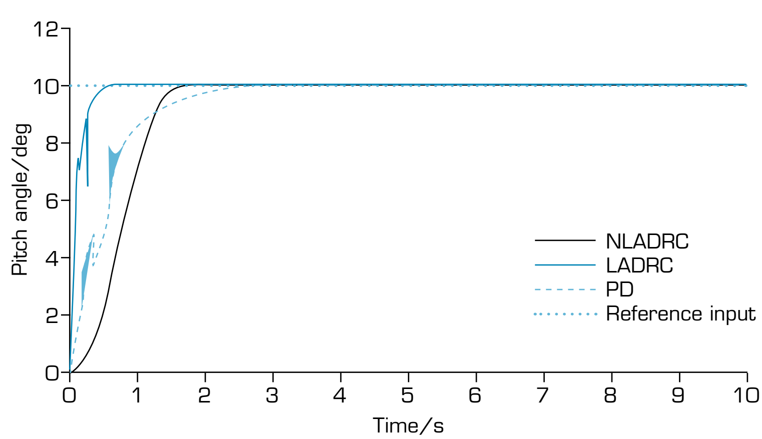

Figure 5. Response curve of yaw channel.

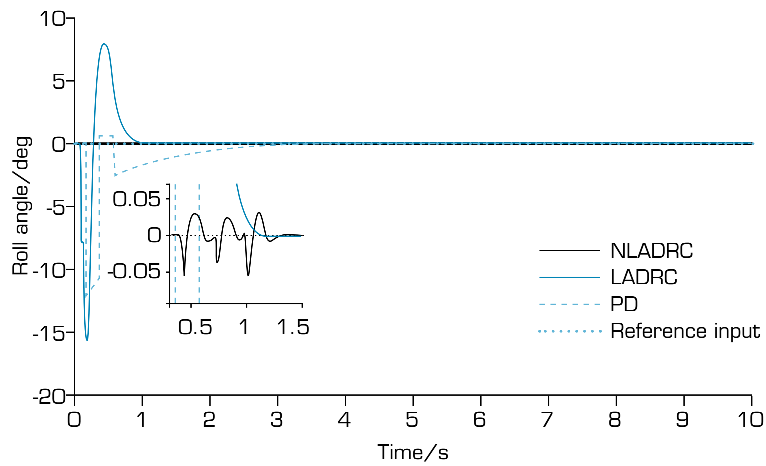

Figure 6. Response curve of rolling channel.

Table 1. Comparison table of three control algorithms without external disturbance and parameter perturbation.

Compare items	Pitch channel			Yaw channel		
	Rise time (s)	Setting time (s)	Overshoot (%)	Rise time (s)	Setting time (s)	Overshoot (%)
PD	0.93	1.58	1.1	1.31	2.30	0
LADRC	0.32	0.52	0	0.27	0.48	0
NLADRC	0.81	1.31	0	0.90	1.47	0

It can be seen from the above figures and table that the PD controller has overshoot in the pitch channel, and the response speed is the slowest. However, LADRC has the fastest response speed, and NLADRC has the middle response speed.

- Verifying the performance of the controller in the presence of external disturbance.

When the external disturbance $d = 5\sin(\frac{\pi}{2}t)$ is added to the three channels of the missile attitude model, the simulation results of three channels are shown in Figs. 7, 8 and 9. And the three control algorithms are compared, as shown in Table 2.

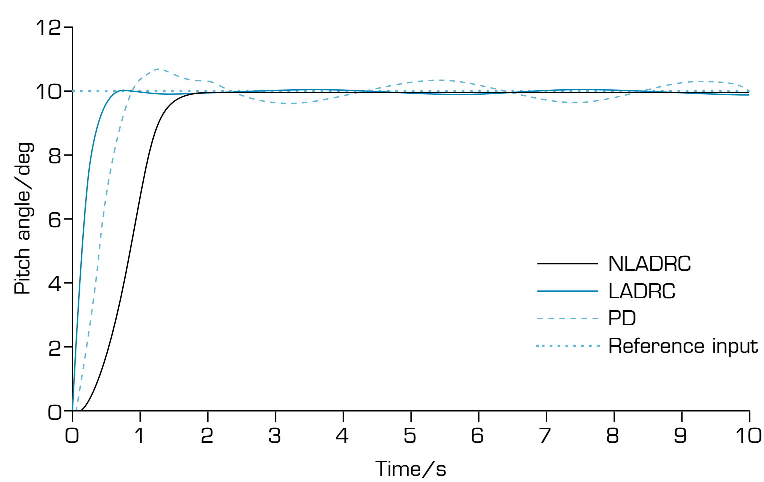

Figure 7. Response curve of pitch channel under external disturbance.

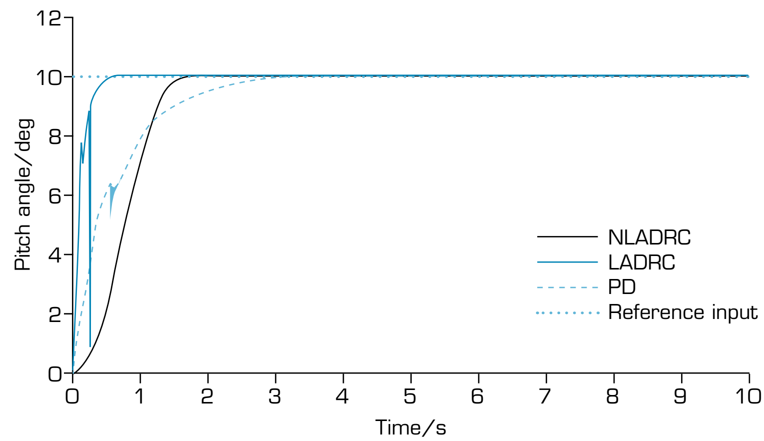

Figure 8. Response curve of yaw channel under external disturbance.

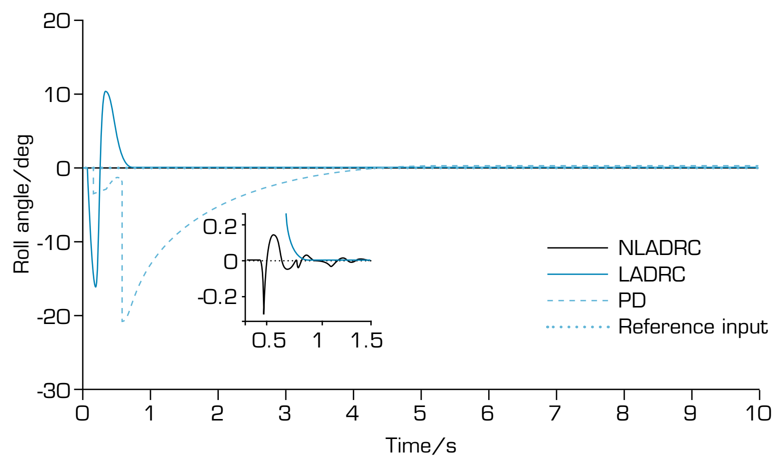

Figure 9. Response curve of rolling channel under external disturbance.

Table 2. Comparison table of three control algorithms in the presence of external disturbances.

Compare items	Pitch channel			Yaw channel		
	Rise time (s)	Setting time (s)	Overshoot (%)	Rise time (s)	Setting time (s)	Overshoot (%)
PD	0.84	2.12	4.9	1.41	2.49	0
LADRC	0.35	0.53	0	0.30	0.50	0
NLADRC	0.90	1.47	0	0.90	1.47	0

It can be seen from Table 2 that the PD controller has a large overshoot in the pitch channel. It cannot suppress interference better. However, compared with the simulation results without external disturbance and parameter perturbation, the response speed of LADRC and NLADRC changes slightly, which can better suppress interference. And it can be seen from Figs. 8 and 9 that NLADRC has stronger anti-interference ability than LADRC.

- Verifying the performance of the controller in the presence of model parameter perturbation.

When the influence of model parameter perturbation is considered, that is, the moment of inertia of the missile to each axis of the missile body coordinate system is biased upward by 20%, the simulation results of three channels are shown in Figs. 10, 11 and 12. And the three control algorithms are compared, as shown in Table 3.

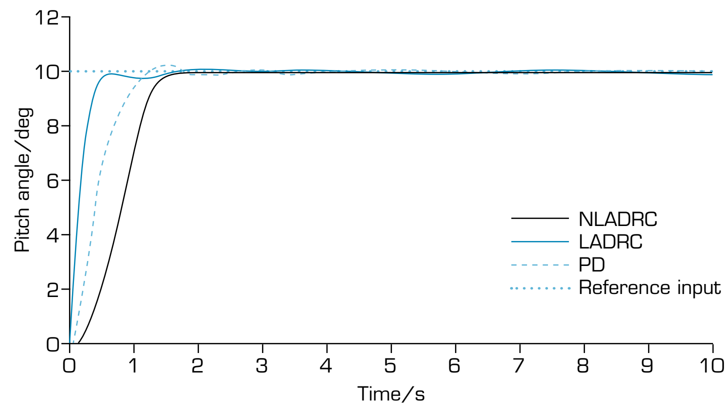

Figure 10. Response curve of pitch channel with parameter perturbation.

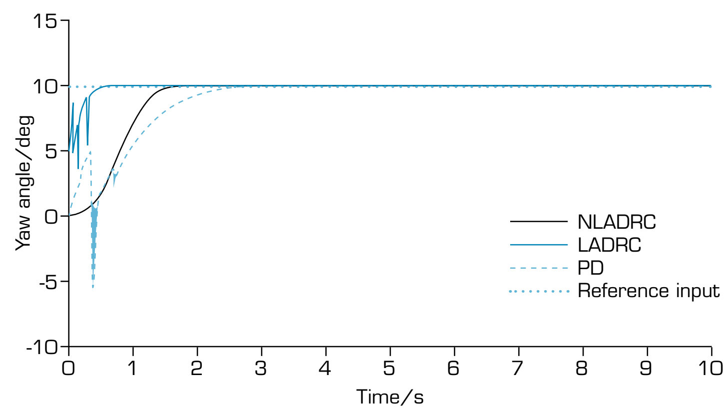

Figure 11. Response curve of yaw channel with parameter perturbation.

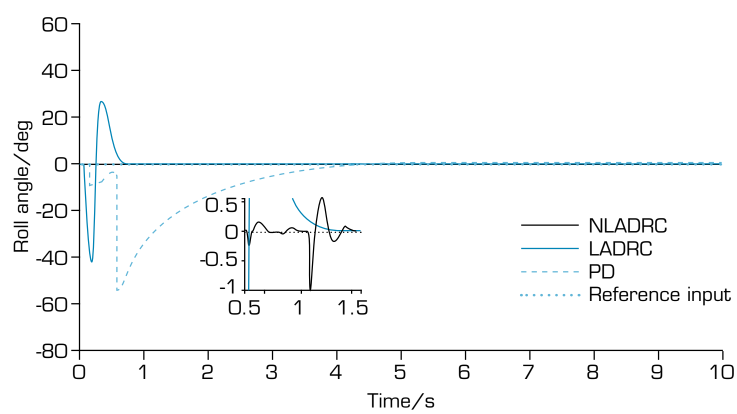

Figure 12. Response curve of rolling channel with parameter perturbation.

Table 3. Comparison table of three control algorithms in the presence of model parameter perturbation.

Compare items	Pitch channel			Yaw channel		
	Rise time (s)	Setting time (s)	Overshoot (%)	Rise time (s)	Setting time (s)	Overshoot (%)
PD	1.19	1.69	0.7	1.86	2.95	0
LADRC	0.39	0.50	0	0.29	0.47	0
NLADRC	0.87	1.44	0	0.90	1.47	0

It can be seen from Table 3 that although the overshoot is reduced in the PD control of the pitch channel, the response speed is slower. However, the response speed of LADRC and NLADRC does not change much compared with the response speed without model parameter perturbation, which can better suppress parameter perturbation. Furthermore, as can be seen from Figs. 11 and 12, NLADRC has better ability to suppress model parameter perturbation than LADRC.

CONCLUSION

In this paper, the nonlinear mathematical model of missile attitude is used as the research object, in which the coupling among the channels is considered. Firstly, the mathematical model of missile attitude is established, and the ADRC method is introduced. Then, the controller of PD, NLADRC and LADRC are designed for the three-channel nonlinear mathematical model of missile in coupling states. Finally, the control performance of the three methods is compared by using MATLAB. The simulation results show that the three methods can achieve stable tracking of the missile's flight attitude with or without external disturbance and parameter perturbation. Besides, NLADRC has no overshoot, which saves more energy when completing the mission with the same flight attitude. Furthermore, when external disturbance and model parameter perturbation are added to the model respectively, the response curve of the system which uses NLADRC method is almost unchanged. NLADRC method has the strongest anti-interference ability and the best robustness. LADRC has the fastest tracking speed, PD control has the slowest tracking speed, and tracking speed of NLADRC is between LADRC and PD control, additionally, the parameter tuning of LADRC is simpler than NLADRC.

In a word, NLADRC and LADRC have their own advantages. In order to take better use of the superiorities of NLADRC, the advantages of the two control methods can be combined, and study the methods of nonlinear and linear switched control to refrain from the shortcomings of nonlinear control.

AUTHORS' CONTRIBUTION

Conceptualization: Liu S and Xue M; **Methodology:** Liu S and Xue M; **Formal Analysis:** Xue M; **Investigation:** Qiu Y, Zhou X and Zhao Q; **Writing – Original Draft:** Xue M; **Writing – Review & Editing:** Liu S and Xue M; **Funding Acquisition:** Liu S; **Resources:** Liu S; **Supervision:** Liu S.

DATA AVAILABILITY STATEMENT

All data sets were generated or analyzed in the current study.

FUNDING

National Natural Science Foundation of China
[https://doi.org/10.13039/501100001809]
Grant No: 61976081.

ACKNOWLEDGEMENTS

Not applicable.

REFERENCES

Basha SM, Swarup A (2017) Disturbance observer based fuzzy PID and robust PID autopilot design for bank-to-turn missile. Paper presented 2017 IEEE 8th International Conference on Computing, Communications and Networking Technologies (ICCCNT). IEEE; IIT Delhi, Delhi, India. https://doi.org/10.1109/ICCCNT.2017.8204122

Chen CB, Liu B, He N, Gao S, Pan Q (2012) PID control based missile sub-channel simulation. Adv Mater Res 433-440:7011-7016. https://doi.org/10.4028/www.scientific.net/AMR.433-440.7011

Chen ZQ, Sun MW, Yang RG (2013) On the stability of linear active disturbance rejection control. Acta Autom Sin 39(5):574-580. Chinese. https://doi.org/10.3724/SP.J.1004.2013.00574

Gao ZQ (2003) Scaling and bandwidth-parameterization based control tuning. Proceedings of the American Control Conference. IEEE; Denver, CO, United States. https://doi.org/10.1109/ACC.2003.1242516

Han JQ (2002) From PID technique to active disturbances rejection control technique. Control Engineering of China 9(3):13-18. Chinese. https://doi.org/10.3969/j.issn.1671-7848.2002.03.003

Han JQ (2008) Active disturbance rejection control technique – the technique for estimating and compensating the uncertainties. Beijing: National Defense Industry Press. Chinese.

Li B, Ma F, Wu Y (2020) Missile attitude control based on deep reinforcement learning. Paper presented 2020 IEEE 16th International Conference on Control and Automation (ICCA). IEEE; Sapporo, Hokkaido, Japan. https://doi.org/10.1109/ICCA51439.2020.9264391

Liu JJ, Hao MR, Sun MW, Guo X, Chen ZQ (2019) PID attitude controller tuning for aerodynamic missile based on reinforcement learning. Tactical Missile Technology 2019(5):58-63. Chinese. https://doi.org/10.16358/j.issn.1009-1300.2019.9.116

Lu KW, Yang Z, Zhang QY, Xu CL, Xu H, Xu XR (2020) Active disturbance rejection flight control method for thrust-vectored quadrotor with tiltable rotors. Control Theory & Applications 37(6):1377-1387. Chinese. https://doi.org/10.7641/CTA.2019.90305

Sun B, Wang HX, Su T, Sheng CY, Lv XR (2020) Nonlinear active disturbance rejection controller design and tuning for permanent magnet synchronous motor speed control system. Proceedings of the CSEE 40(20):6715-6726. Chinese. https://doi.org/10.13334/j.0258-8013.pcsee.200018

Xu Q, Wang X, Wu J, Song YP, Zhang R (2018) Attitude control of missile based on extended state observer and command filter. Flight Dynamics 36(1):52-55. Chinese. https://doi.org/10.13645/j.cnki.f.d.20170825.001

Yuan D, Ma XJ, Zeng QH, Qiu XB (2013) Research on frequency-band characteristics and parameters configuration of linear active disturbance rejection control for second-order systems. Control Theory & Applications 30(12):1630-1640. Chinese. https://doi.org/10.7641/CTA.2013.30424

Zhou D (2002) New guidance laws for homing missiles. Beijing: National University of Defense Technology Press. Chinese.